Available online at www.sciencedirect.com

SciVerse ScienceDirect

Ceramics International 38 (2012) 5925–5930

CERAMICS INTERNATIONAL

www.elsevier.com/locate/ceramint

TiO_2 nanofibers doped with rare earth elements and their photocatalytic activity

M. Shamshi Hassan [a], Touseef Amna [b], O-Bong Yang [c], Hyun-Chel Kim [d], Myung-Seob Khil [a,*]

[a] Department of Organic Materials and Fiber Engineering, Chonbuk National University, Jeonju 561-756, Republic of Korea
[b] Center for Healthcare Technology Development, Chonbuk National University, Jeonju 561-756, Republic of Korea
[c] School of Semiconductor and Chemical Engineering, Chonbuk National University, Jeonju 561-756, Republic of Korea
[d] Korean Institute for Knit Industry, Iksan 570-330, Republic of Korea

Received 22 March 2012; received in revised form 13 April 2012; accepted 13 April 2012
Available online 20 April 2012

Abstract

In the present study rare earth doped (Ln^{3+}–TiO_2, Ln = La, Ce and Nd) TiO_2 nanofibers were prepared by the sol–gel electrospinning method and characterized by XRD, SEM, EDX, TEM, and UV-DRS. The photocatalytic activity of the samples was evaluated by Rhodamine 6G (R6G) dye degradation under UV light irradiation. XRD analysis showed that all the synthesized pure and doped titania nanofibers contain pure anatase phase at 500 °C but at 700 °C it shows both anatase and rutile phase. XRD result also shows that Ln^{3+}-doped titania probably inhibits the phase transformation. The diameter of nanofibers for all samples ranges from 200 to 700 nm. It was also observed that the presence of rare-earth oxides in the host TiO_2 could decrease the band gap and accelerate the separation of photogenerated electron–hole pairs, which eventually led to higher photocatalytic activity. To sum up, our study demonstrates that Ln^{3+}-doped TiO_2 samples exhibit higher photocatalytic activity than pure TiO_2 whereas Nd^{3+}-doped TiO_2 catalyst showed the highest photocatalytic activity among the rare earth doped samples.

Keywords: Ln-doped titania; Electrospinning; Nanofibers; Dye degradation

1. Introduction

Among various semiconductors titania is widely used photocatalyst due to its strong oxidizing power, stable at different pH and favorable band gap energy. However titania also has some disadvantages like low surface area, fast recombination and wavelength maximum lies in UV region. Adsorption behavior and the separation efficiency of electron–hole pairs are two important factor on which photodegradation of TiO_2 strongly depends [1]. High specific surface area of catalysts generally increases the adsorption efficiency. Surface recombination can be avoided by transition metals doping [2], coupling with other semiconductors [3], noble metals deposition [4] and rare earth ions doping [5,6], whereas, volume recombination can be reduced by preparing titania in nanoscale. In recent years, many groups have examined the effect of metal doping on photocatalytic properties of TiO_2. Doping with lanthanides is a method to shift the maximum of absorption as well as enhance the photocatalytic activity. In addition to the methods of catalyst preparation, the photoactivity of the doped TiO_2 catalysts depends substantially on the nature of the dopant and its concentration [7].

One dimensional porous titania nanofibers consisting of well crystallized anatase nanocrystals is very advantageous for developing active photocatalytic materials for environmental purification and green energy [8]. Such materials are usually having large surface area and high porosity. A larger surface area provides more surface active sites for the adsorption of reactants molecules, which thus make the photocatalytic process more efficient [9]. Nanofibers have large surface area and regular morphology on nanometer scale. Due to their one dimensional morphology, the nanofibers sediment readily from their aqueous dispersions, compared with P25.

In order to investigate the light absorption ability of TiO_2 doped with different lanthanum metal and the effects of doping on the photocatalytic activity, the present work was designed to prepare Ln-doped TiO_2 nanofibers by electrospinning and characterized by XRD, TEM, and DRS patterns. Finally,

* Corresponding author. Tel.: +82 63 270 4635; fax: +82 63 270 4249.
E-mail address: mskhil@jbnu.ac.kr (M.-S. Khil).

0272-8842/$36.00
http://dx.doi.org/10.1016/j.ceramint.2012.04.043

pristine and doped TiO_2 were tested for photocatalytic degradation of R6G.

2. Experimental details

In a typical procedure [10], PVAc solution (18 wt%) was prepared by dissolving PVAc in DMF (2,2-dimethyl formamide) under magnetic stirring for 6 h. 5 g of titanium isopropoxide (TTIP) was taken in a separate bottle and add a few drops of acetic acid till the solution became transparent. Appropriate amount (1.0 wt%) of alcoholic solution of $Ln(NO_3)_3$ was added into the TTIP solution. Then 6 g of PVAc solution was mixed slowly into TTIP under vigorous stirring. The obtained solution was put in a 10 ml syringe with a stainless steel needle. A copper pin connected to a high voltage generator was inserted in the solution as a positive terminal whereas a ground iron drum covered by polyethylene sheet served as counter electrode. The distance between the syringe needle tip and collector was fixed at 18 cm at 15 kV. The as synthesized mat of composite fiber was initially dried at 80 °C for 24 h under vacuum, and then calcined at 500 and 700 °C for 2 h in air atmosphere with a heating rate of 2 °C/min.

The crystallinity of pristine TiO_2 and Ln-doped TiO_2 catalysts were analyzed by X-ray powder diffraction recorded on a Rigaku/Max-3A X-ray diffractometer with CuKα radiation (λ = 1.540 Å). To examine the microstructure, the synthesized products were characterized by scanning electron microscopy (SEM, JEOL JSM6700, Japan) and transmission electron microscope (TEM, JEOL JEM-2010). The light absorbance of the samples was measured by using UV–vis diffused reflectance spectrum (UV-DRS, 525 Shimadzu).

The photocatalytic degradation was carried out by mixing 15 mg of the pure TiO_2 or Ln-doped TiO_2 photocatalysts into the 100 ml of (10 ppm) R6G aqueous solution under continuous stirring. The experiments were performed at room temperature and prior to irradiation, the slurry was aerated for 30 min to reach adsorption equilibrium followed by UV irradiation. Aliquots were withdrawn from the suspension at specific time intervals and centrifuged immediately at 12,000 rpm. The absorbance of the R6G solution was measured with a UV–vis spectrophotometer (Shimadzu UV-3101).

3. Results and discussion

Fig. 1 shows the XRD patterns of pure and Ln-doped titania samples at 500 °C. The crystalline phase of all pure and doped titania is showing the anatase phase [11] at 500 °C. Xu et al. [12] reported that rare earth metal salts can be changed into rare earth oxides (La_2O_3) during the calcination process. Therefore, it can be inferred that the Ln^{3+} ions were dispersed on the surface of TiO_2 in the form of small Ln_2O_3 clusters. When the samples were calcined at 700 °C, the XRD spectra show the presence of rutile phase in addition to anatase phase (Fig. 2). It can be seen that the intensity of anatase phase decreased, while the intensity of rutile phase increased as the temperature was raised. The percentage of anatase (X_A) in the sample can be estimated from the respective integrated XRD peak intensity

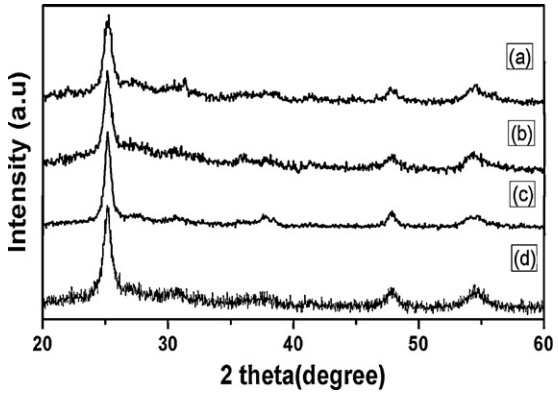

Fig. 1. XRD pattern of (a) TiO_2, (b) La–TiO_2, (c) Ce–TiO_2, and (d) Nd–TiO_2 nanofibers at 500 °C.

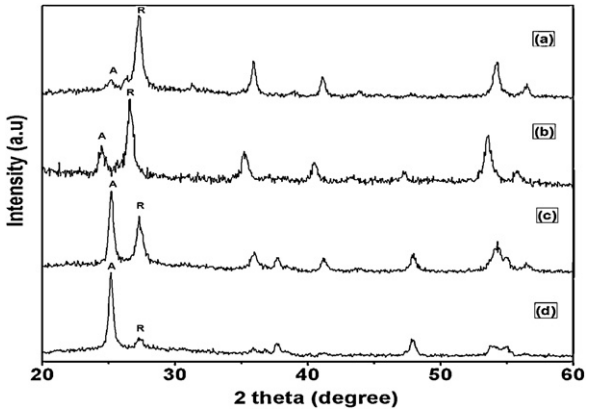

Fig. 2. XRD pattern of (a) TiO_2, (b) La–TiO_2, (c) Ce–TiO_2, and (d) Nd-TiO_2 nanofibers at 700 °C.

using the following equation [13], X_A (%) = 100/(1 + 1.265I_R/I_A), where I_A represents the intensity of anatase peak and I_R is the intensity of rutile peak and X_A is the weight percentage of anatase in the sample. The percentage of rutile phase is more in bare titania than lanthanide ion doped titania (Table 1). From this result may say that Ln^{3+} doping probably inhibits the phase transformation. From the (1 0 1) peak of anatase TiO_2 at 500 °C, the average size of crystallite (D) was calculated (Table 1) using the Scherrer equation: $D = K\lambda/\beta \cos\theta$ where β is the full width half maximum (FWHM) of the 2θ peak, K is the shape factor of the particles (it equals to 0.95), θ and λ are the incident angle and the wavelength of the X-rays, respectively. However, no diffraction peaks of rare earth oxides appeared even when the samples were calcined at 700 °C, which might be because the content of rare earth oxides was below the detection limit of XRD analysis and large difference between the ionic radii of Ti^{4+} lanthanide ions (Ln^{3+}) [14].

Table 1
Comparison of properties of titania and doped titania nanofibers.

Sample	TiO_2	TiO_2–La	TiO_2–Ce	TiO_2–Nd
B.Gap (eV)	3.48	3.17	3.14	3.1
Cryst. size (nm)	29.54	12.51	11.49	10.2
X_A (%)	12.5	35	62.5	86.8

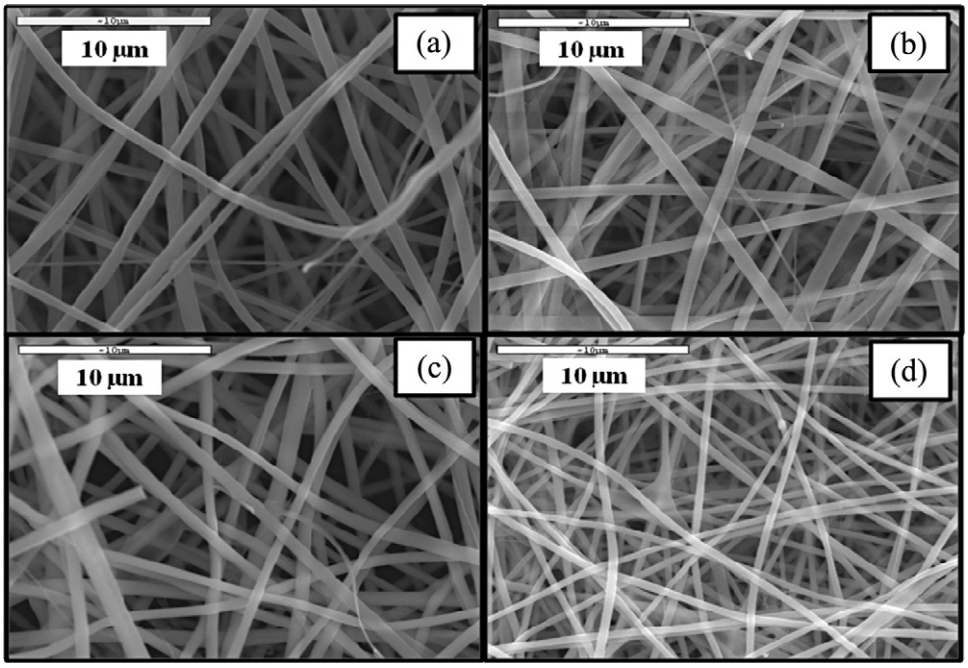

Fig. 3. SEM micrographs of (a) TiO_2, (b) La–TiO_2, (c) Ce–TiO_2, and (d) Nd–TiO_2 nanofibers.

The SEM images of the synthesized TiO_2 and rare earth doped TiO_2 photocatalyst samples are shown in Fig. 3. Each individual nanofiber has smooth surface morphology and uniform diameter. Fig. 4 shows the energy-dispersive X-ray spectroscopy (EDX) analysis of the Ln-doped titania nanofibers. It has been observed that the sample contains Ti, Ln (Ln = Nd, Ce, La) and O; no other element impurity is detected, indicating the final product is free of impurity and composed of Ln_2O_3 and TiO_2. The microstructures of the nanofibers were further investigated by TEM. Fig. 5 shows typical TEM images of pristine and doped titania nanofibers at 700 °C. Typical porous structures of the nanofibers were observed which is known to possess superior photocatalytic activity. The average nanofibers diameter of all the samples was found to be around 250 nm, 260 nm, 700 nm and 340 nm for TiO_2, La–TiO_2, Ce–TiO_2 and Nd–TiO_2 respectively. According to the crystal lattice parameters, Ln_2O_3 and TiO_2 cannot combine in a single crystal. Accordingly, a main TiO_2 nanofiber doped with Ln_2O_3 nanoparticles is the expected structure of the obtained product. To affirm this hypothesis, HR-TEM analysis of Nd-doped TiO_2

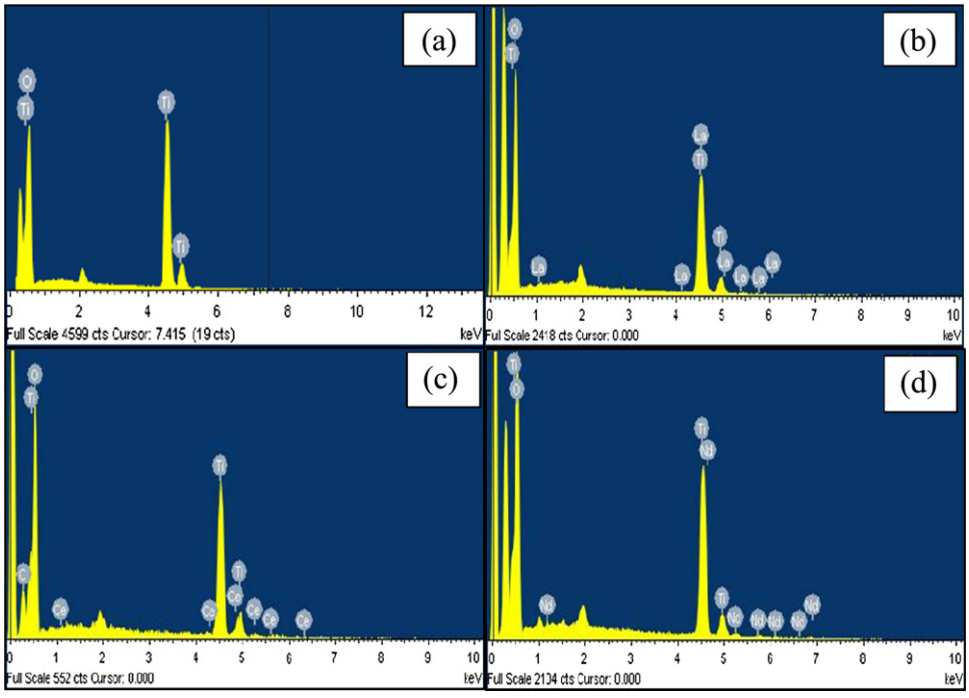

Fig. 4. EDX spectra of (a) TiO_2, (b) La–TiO_2, (c) Ce–TiO_2, and (d) Nd–TiO_2 nanofibers.

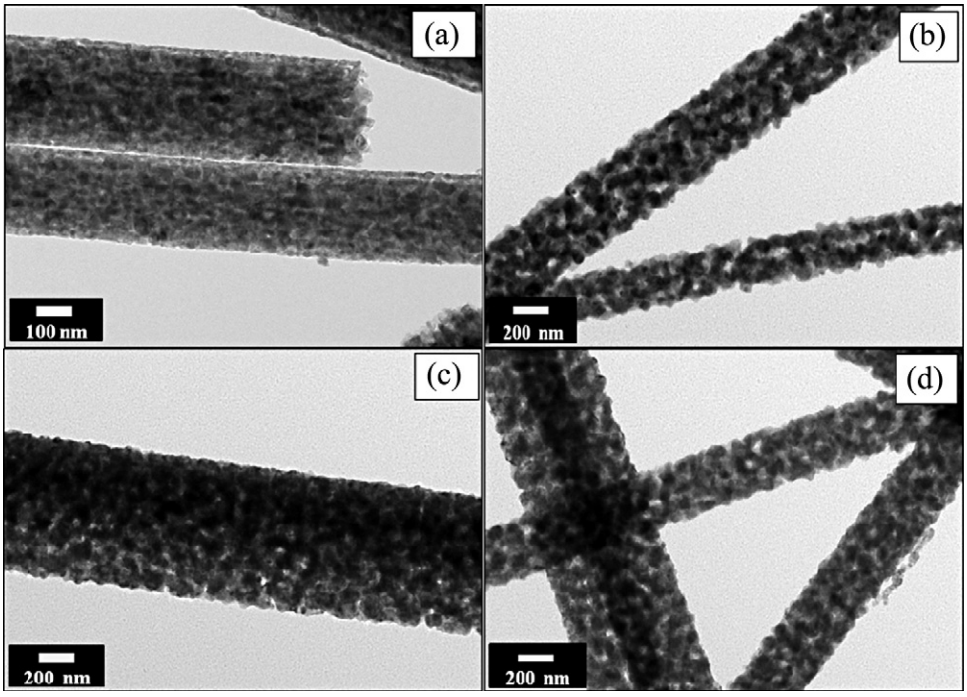

Fig. 5. TEM micrographs of (a) TiO_2, (b) La–TiO_2, (c) Ce–TiO_2, and (d) Nd–TiO_2 nanofibers.

has been conducted (Fig. 6). As shown in the HR-TEM image (Fig. 6), the black nanoparticles do have different crystal lattice parameters than the matrix as the crystal plane are closer, so one can claim that these nanoparticles represent Nd_2O_3. Moreover, the selected area electron diffraction (SAED) pattern confirms the good crystallinity of the sample (inset Fig. 6).

The DRS spectra of pure TiO_2 and Ln^{3+}-doped TiO_2 samples calcined at 700 °C are shown in Fig. 7. In comparison with those of pure TiO_2, the optical absorption edges of the Ln^{3+}–TiO_2 samples are shifted toward longer wavelength in the order of Nd^{3+}–TiO_2 > Ce^{3+}–TiO_2 > La^{3+}–TiO_2 > TiO_2 photocatalyst. This red shift in the optical absorption band is due to the presence of the rare-earth ions, and it can be attributed to a charge-transfer transition between the lanthanide f electrons and the conduction or valence band of the host TiO_2 [15]. Compared with the other Ln^{3+}–TiO_2 samples, the Nd^{3+}–TiO_2 photocatalyst had the highest absorption intensity and largest red shift, which indicates that the doping of Nd^{3+} should have the best photoresponse in the UV region, as well as the highest photocatalytic activity.

To investigate the photocatalytic activities of the Ln-doped titania samples, photocatalytic degradation experiments were carried out using R6G in an aqueous suspension under UV light irradiation. Fig. 8 shows the results of the photocatalytic degradation of R6G in presence of different rare earth doped TiO_2 catalysts with the same dopant content (1.0 wt%) for 60 min of irradiation. The different rare earth loaded photocatalysts exhibited higher photocatalytic degradation activities than pure TiO_2, indicating the promoting effect of the rare earth modification. It has been reported in the literature that the photocatalytic activities of catalysts depend on many factors, such as crystallinity, surface properties, absorption

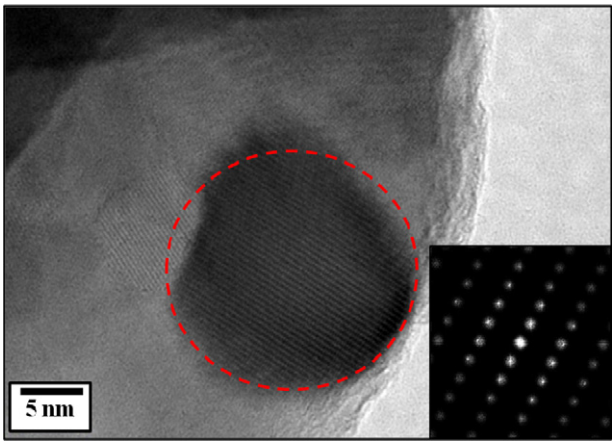

Fig. 6. High resolution TEM (HR-TEM) of Nd-doped TiO_2, the inset shows its SAED pattern.

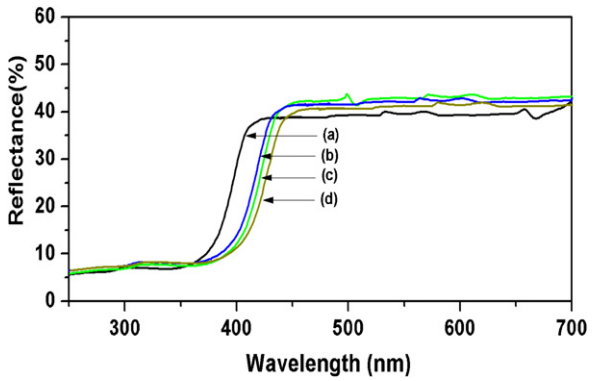

Fig. 7. UV–vis DRS spectra of (a) TiO_2, (b) La–TiO_2, (c) Ce–TiO_2, and (d) Nd–TiO_2 nanofibers.

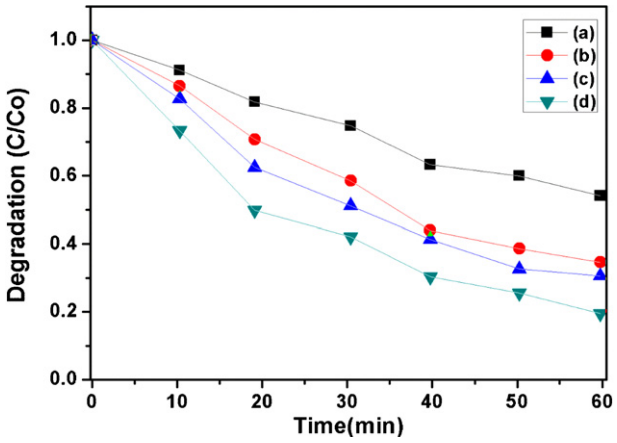

Fig. 8. Photocatalytic degradation of R6G over the different rare earth-doped TiO_2 catalysts (a) TiO_2, (b) La–TiO_2, (c) Ce–TiO_2, and (d) Nd–TiO_2 nanofibers with the same doped contents (1.0 wt%).

properties, and so on [16]. In this case, the enhanced photocatalytic activity of Ln^{3+}–TiO_2 can be explained that the presence of rare earth ions shifts the absorption edge to a longer wavelength in the order Nd^{3+}–$TiO_2 > Ce^{3+}$–$TiO_2 > La^{3+}$–$TiO_2 > TiO_2$ (Fig. 7), which is in consistent with the order of the photocatalytic performances. A larger red shift indicates that a sample can absorb more photons. Therefore, the red shift in the absorption band is favorable for photocatalytic reaction. Our findings are in good agreement with the results of Fan et al. [17] and Zhang et al. [18]. Moreover, for Ln^{3+}-doped TiO_2 samples, the presence of lanthanide ions could increase the interfacial charge transfer and inhibit the recombination of electron–hole pairs. As for the rare earth modified TiO_2 photocatalysts, lanthanide ions could act as effective electron scavengers to trap the conduction band electrons of TiO_2 [19]. In the presence of lanthanide loaded TiO_2 catalysts, the rare earth oxides present on the surface of the host TiO_2 could act as electron traps, which could enhance electron–hole separation and increase the quantum efficiency. Therefore, the photogenerated electrons could easily transfer from the interior to the surface of the catalyst, which would promote photocatalytic reaction.

On the basis of the above analysis, it is suggested that the enhanced photocatalytic activity of rare earth doped TiO_2 could be a synergetic effect of many factors, including red shifts to longer wavelengths, and enhanced rates of interfacial charge transfer. In the present study, it is worth mentioning that Nd^{3+}-doped TiO_2 exhibited the highest dye degradation (~80%) among all photocatalysts. This may be attributed to the high percentage of anatase phase in the sample (Table 1) which is considered to have better photocatalytic activity than the rutile phase [20] and largest red-shift in the optical absorption band were exhibited by the Nd^{3+}-loaded TiO_2 (Fig. 7).

Previously, the detailed mechanisms involved in semiconductor photocatalysis have been studied and reviewed [21–24]. Usually it is considered that the process is initiated by the band-gap excitation of TiO_2 under UV illumination ($\lambda < 385$ nm). Excited by energetic photons, electrons (e^-) are transferred from the valence band to the conduction band of TiO_2, thus generating a hole (h^+) in the valence band (Eq. (1)). The electrons and holes diffuse to the surface of TiO_2 and react with the adsorbed O_2, water and surface hydroxide group, respectively, leading to the production of O_2^- (Eq. (2)) and $^\bullet OH$ (Eqs. (3) and (4)). The resulting $^\bullet OH$ radical, being a very strong oxidizing agent (standard redox potential +2.8 V) can oxidize dyes to the mineral end-products. According to this, the relevant reactions at the semiconductor surface causing the degradation of dyes can be expressed as follows:

$$TiO_2 + h\upsilon(UV) \rightarrow TiO_2(h_{vb}{}^+ + e_{cb}{}^-) \quad (1)$$

$$TiO_2(e_{cb}{}^-) + O_2 \rightarrow TiO_2 + O_2{}^{\bullet -} \quad (2)$$

$$TiO_2(h_{vb}{}^+) + H_2O \rightarrow TiO_2 + {}^\bullet OH + H^+ \quad (3)$$

$$TiO_2(h_{vb}{}^+) + OH^- \rightarrow TiO_2 + {}^\bullet OH \quad (4)$$

$$O_2{}^{\bullet -} \text{or} {}^\bullet OH + R6G \rightarrow \text{degradationproduct} \quad (5)$$

where $h\upsilon$ is photon energy required to excite the semiconductor electron from the valence band (VB) region to conduction band (CB) region.

4. Conclusions

Pure and Ln-doped TiO_2 nanofibers were successfully synthesized by sol–gel electrospinning method and were assayed for photocatalytic activity. Ln^{3+}-doped TiO_2 samples were found to exhibit higher photocatalytic activities than pure TiO_2 because of the synergetic effect of red shifts to longer wavelengths and specific characteristics of lanthanide ions. Nd^{3+}-doped TiO_2 showed the highest activity among all the rare earth doped samples studied.

Acknowledgments

This work was supported by the Industrial Strategic Technology Development Program, 10037345, funded by the Ministry of Knowledge Economy (MKE, Korea).

References

[1] A. Fujishima, T.N. Rao, D.A. Truk, Titanium dioxide photocatalysis, Journal of Photochemistry and Photobiology C: Photochemistry Review 1 (2000) 1–21.
[2] L.G. Devi, S.G. Kumar, Influence of physicochemical–electronic properties of transition metal ion doped polycrystalline titania on the photocatalytic degradation of Indigo Carmine and 4-nitrophenol under UV/solar light, Applied Surface Science 257 (2011) 2779–2790.
[3] C. Wang, B.Q. Xu, X. Wang, J. Zhao, Preparation and photocatalytic activity of ZnO/TiO_2/SnO_2 mixture, Journal of Solid State Chemistry 178 (2005) 3500–3506.
[4] F.B. Li, X.Z. Li, Photocatalytic properties of gold/gold ion-modified titanium dioxide for wastewater treatment, Applied Catalysis A: General 228 (2002) 15–27.
[5] Y. Zhang, H. Xu, Y. Xu, H. Zhang, Y. Wang, The effect of lanthanide on the degradation of RB in nanocrystalline Ln/TiO_2 aqueous solution, Journal of Photochemistry and Photobiology A: Chemistry 170 (2005) 279–285.
[6] X. Yan, J. He, D.G. Evans, X. Duan, Y. Zhu, Preparation characterization and photocatalytic activity of Si-doped and rare earth doped TiO_2 from

mesoporous precursors, Applied Catalysis B: Environmental 55 (2005) 243–252.
[7] J.A. Navio, J.J. Testa, P. Djedjeian, J.R. Padron, D. Rodriguez, M.I. Litter, Iron-doped titania powders prepared by a sol–gel method. Part II. Photocatalytic properties, Applied Catalysis A: General 178 (1999) 191–203.
[8] J.G. Yu, H.T. Guo, S.A. Davis, S. Mann, Fabrication of hollow inorganic microspheres by chemically induced self-transformation, Advanced Functional Materials 16 (2006) 2035–2041.
[9] Y. Zhang, G. Li, Y. Wu, Y. Luo, L. Zhang, The formation of mesoporous TiO_2 spheres via a facile chemical process, Journal of Physical Chemistry B 109 (2005) 5478–5481.
[10] T. Amna, M.S. Hassan, A. Yousef, A. Mishra, N.A.M. Barakat, M.S. Khil, H.Y. Kim, Inactivation of foodborne pathogens by NiO/TiO_2 composite nanofibers: a novel biomaterial system, Food and Bioprocess Technology, 2011, http://dx.doi.org/10.1007/s11947-011-0741-1, in press.
[11] P. Sorapong, S. Yoshikazu, S. Yoshikawa, R. Kawahata, Synthesis of titanate TiO_2 (B), and anatase TiO_2 nanofibers from natural rutile sand, Journal of Solid State Chemistry 178 (2005) 3110–3116.
[12] A.W. Xu, Y. Gao, H.Q. Liu, The preparation, characterization, and their photocatalytic activities of rare-earth-doped TiO_2 nanoparticles, Journal of Catalysis 207 (2002) 151–157.
[13] Q.H. Zhang, L. Gao, J.K. Guo, Effects of calcination on the photocatalytic properties of nanosized TiO_2 powders prepared by $TiCl_4$ hydrolysis, Applied Catalysis B 26 (2000) 207–215.
[14] R.D. Shannon, Revised effective ionic radii and systematic studies of interatomic distances in halides and chalcogenides, Acta Crystallographica Section A: Crystal Physics, Diffraction, Theoretical and General Crystallography 32 (1976) 751–767.
[15] E. Borgarello, J. Kiwi, M. Gratzel, E. Pelizzetti, M. Visca, Visible light induced water cleavage in colloidal solutions of chromium-doped titanium dioxide particles, Journal of the American Chemical Society 104 (1982) 2996–3002.
[16] M. Saif, M.S.A. Abdel-Mottaleb, Titanium dioxide nanomaterial doped with trivalent lanthanide ions of Tb, Eu and Sm: preparation, characterization and potential applications, Inorganica Chimica Acta 360 (2007) 2863–2874.
[17] C. Fan, P. Xue, Y. Sun, Preparation of nano-TiO_2 doped with cerium and its photocatalytic activity, Journal of Rare Earths 24 (2006) 309–313.
[18] Y. Zhang, H. Zhang, Y. Xu, Y. Wang, Significant effect of lanthanide doping on the texture and properties of nanocrystalline mesoporous TiO_2, Journal of Solid State Chemistry 177 (2004) 3490–3498.
[19] F.B. Li, X.Z. Li, M.F. Hou, K.W. Cheah, W.C. Choy, Enhanced photocatalytic activity of Ce^{3+}–TiO_2 for 2-mercaptobenzothiazole degradation in aqueous suspension for odour control, Applied Catalysis A: General 285 (2005) 181–189.
[20] M. Andersson, L. Österlund, S. Ljungström, A. Palmqvist, Preparation of nanosize anatase and rutile TiO_2 by hydrothermal treatment of microemulsions and their activity for photocatalytic wet oxidation of phenol, Journal of Physical Chemistry B 106 (2002) 10674–10679.
[21] M.A. Fox, M.T. Dulay, Heterogeneous photocatalysis, Chemical Reviews 93 (1993) 341–357.
[22] M.R. Hoffmann, S.T. Martin, W. Choi, D.W. Bahnemann, Environmental applications of semiconductor photocatalysis, Chemical Reviews 95 (1995) 69–96.
[23] R.F. Howe, Recent development in photocatalysis, Developments in Chemical Engineering and Mineral Processing 6 (1/2) (1998) 55–84.
[24] I.K. Konstantinou, T.A. Albanis, TiO2-assisted photocatalytic degradation of azo dyes in aqueous solution: kinetic and mechanistic investigations—a review, Applied Catalysis B: Environmental 49 (2004) 1–14.